Electronic Supplementary Material (ESI) for Physical Chemistry Chemical Physics.

Supporting Information (SI)

Multi-Electron Reduction of Wells-Dawson Polyoxometalate Films onto Metallic, Semiconducting and Dielectric Substrates

Antonios M. Douvas,[1,] Dimitris Tsikritzis,[2] Charalampos Tselios,[2] Ali Haider,[3,4] Ali S. Mougharbel,[3] Ulrich Kortz,[3] Anastasia Hiskia,[1] Athanassios G. Coutsolelos,[5] Leonidas C. Palilis,[6] Maria Vasilopoulou,[1] Stella Kennou,[2] Panagiotis Argitis[1]*

[1]*Institute of Nanoscience and Nanotechnology (INN), National Center for Scientific Research (NCSR) "Demokritos", 15341 Agia Paraskevi, Attica, Greece*

[2]*Department of Chemical Engineering, University of Patras, 26504 Rio Patras, Greece*

[3]*Department of Life Sciences & Chemistry, Jacobs University Bremen, 28759 Bremen, Germany*

[4]*Department of Chemistry, Quaid-e-Azam University, 45320 Islamabad, Pakistan*

[5]*Department of Chemistry, University of Crete, Voutes Campus, 70013 Heraklion, Crete, Greece*

[6]*Department of Physics, University of Patras, 26504 Rio Patras, Greece*

[*]Correspondence to: Dr. A. M. Douvas (e-mail: a.douvas@inn.demokritos.gr)

Table of Contents

Figure S6. UV-Vis monitoring of a thick $(NH_4)_6P_2Mo_{18}O_{62}$ film, a thick $(NH_4)_6P_2W_{18}O_{62}$ film, and a thin $H_4SiW_{12}O_{40}$ film, onto Al-coated quartz slides, upon increase of thermal treatment temperature.

Figure S7. UV-Vis spectra of thin POM films onto bare quartz slides: (a) $H_3PW_{12}O_{40}$ film, (b) $H_3PMo_{12}O_{40}$ film, (c) $(NH_4)_6P_2W_{18}O_{62}$ film, and (d) $(NH_4)_6P_2Mo_{18}O_{62}$ film.

Table S1. Energy levels values of POMs deduced from the corresponding UPS spectra and UV-Vis spectra of POMs.

Figure S8. XPS spectrum of a thick $(NH_4)_6P_2Mo_{18}O_{62}$ film onto SiO_2-coated Si wafer.

Figure S9. UV-Vis monitoring of a thin $(NH_4)_6P_2W_{18}O_{62}$ film, a thin $H_4SiW_{12}O_{40}$ film, and a thick $(NH_4)_6P_2Mo_{18}O_{62}$ film onto bare quartz slides, upon increase of thermal treatment temperature.

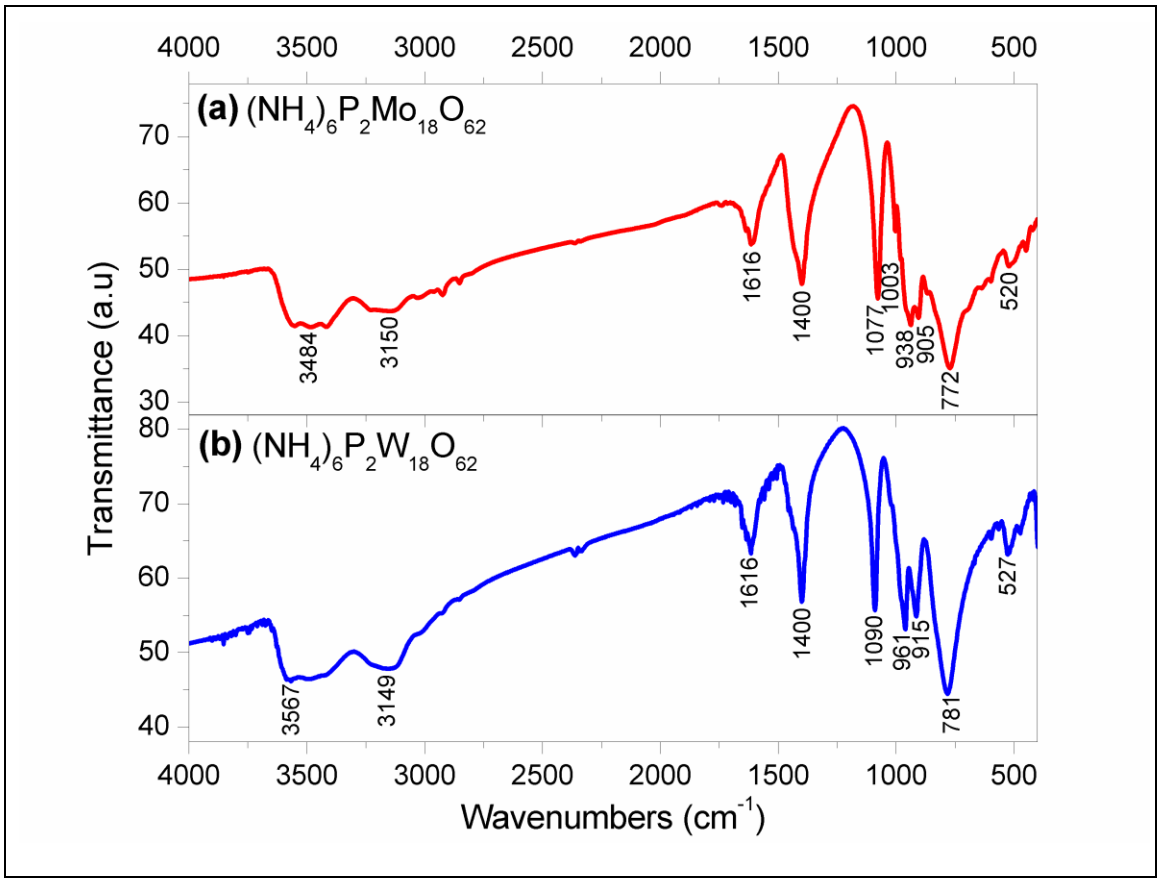

Figure S1. FT-IR spectra of $(NH_4)_6P_2Mo_{18}O_{62}$ and $(NH_4)_6P_2W_{18}O_{62}$ (1% in KBr pellets).

FT-IR peaks of $(NH_4)_6P_2Mo_{18}O_{62}$ (Fig. S1a): 3484 and 3150 cm^{-1}, strong, broad bands attributed to N–H stretching vibrations (non-bonded, antisymmetric and symmetric; ν_{as} and ν_s respectively) of NH_4^+ cations; 1616 and 1400 cm^{-1}, strong, broad bands ascribed to N–H bending vibrations (antisymmetric and symmetric; δ_{as} and δ_s respectively) of NH_4^+ cations; 1077 cm^{-1}, ν_{as} of P–O_a bonds; 1003 and 938 cm^{-1}, ν_s and ν_{as} of Mo=O_d bonds respectively; 905 cm^{-1}, ν_{as} of Mo–O_b–Mo bridges; 772 cm^{-1}, ν_{as} of Mo–O_c–Mo bridges.[36-41,44]

FT-IR peaks of $(NH_4)_6P_2W_{18}O_{62}$ (Fig. S1b): 3567 and 3149 cm^{-1}, strong, broad bands attributed to ν_{as} and ν_s of N–H bonds of NH_4^+ cations respectively; 1616 and 1400 cm^{-1}, strong, broad bands ascribed to δ_{as} and δ_s of N–H bonds of NH_4^+ cations respectively; 1090 cm^{-1}, ν_{as} of P–O_a bonds; 961 cm^{-1}, ν_{as} of W=O_d bonds; 915 cm^{-1}, ν_{as} of W–O_b–W bridges; 781 cm^{-1}, ν_{as} of W–O_c–W bridges.[38,40,44-46]

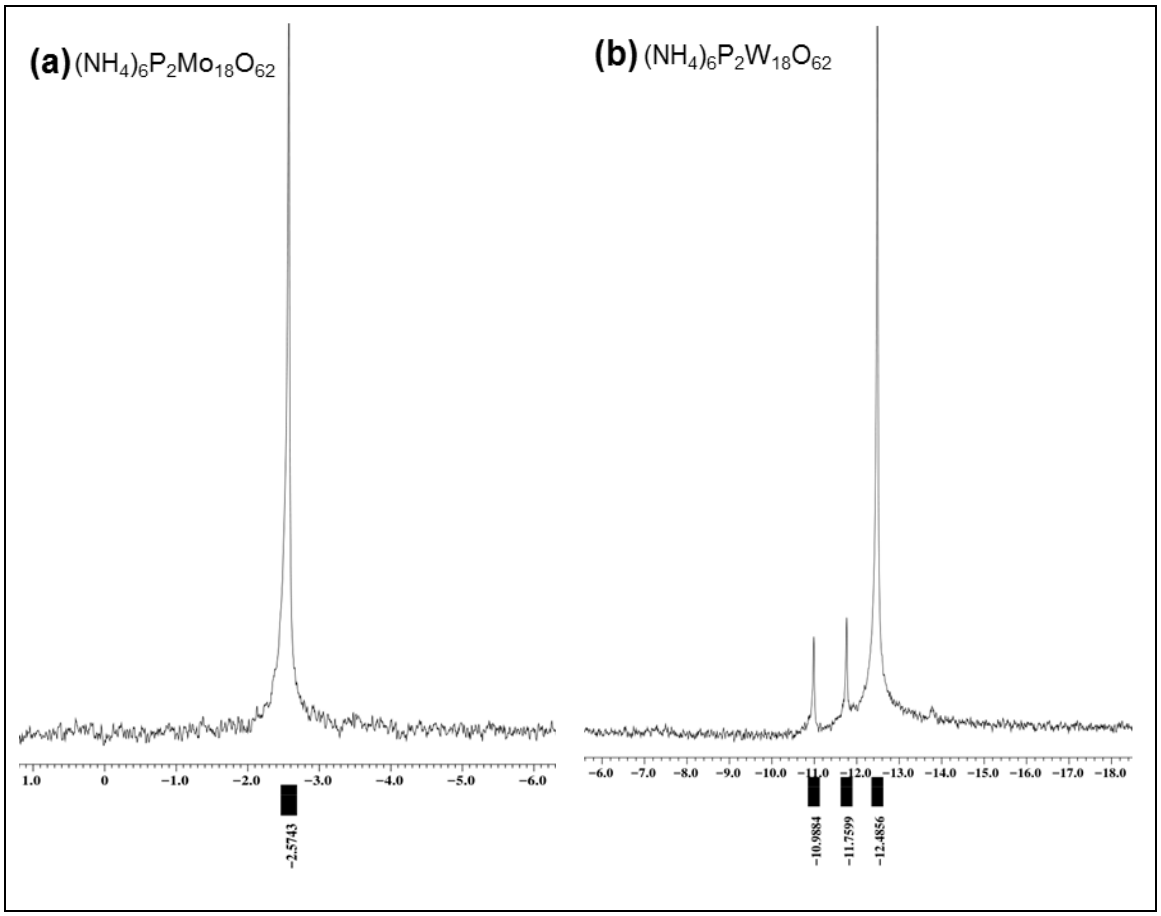

Figure S2. ^{31}P NMR spectra of $(NH_4)_6P_2Mo_{18}O_{62}$ and $(NH_4)_6P_2W_{18}O_{62}$ (in D_2O).

^{31}P NMR peaks of $(NH_4)_6P_2Mo_{18}O_{62}$ (Fig. S2a): a single peak with high intensity at -2.5743 ppm attributed to $[P_2Mo_{18}O_{62}]^{6-}$ anion, indicating only one component.[41-43]

^{31}P NMR peaks of $(NH_4)_6P_2W_{18}O_{62}$ (Fig. S2b): a peak with high intensity peak at -12.4856 ppm attributed to α-$[P_2W_{18}O_{62}]^{6-}$ isomer (~95% of total amount);[42,47] two small peaks at -10.9884 and -11.7999 ppm attributed to β-$[P_2W_{18}O_{62}]^{6-}$ isomer (<5%).[42,48]

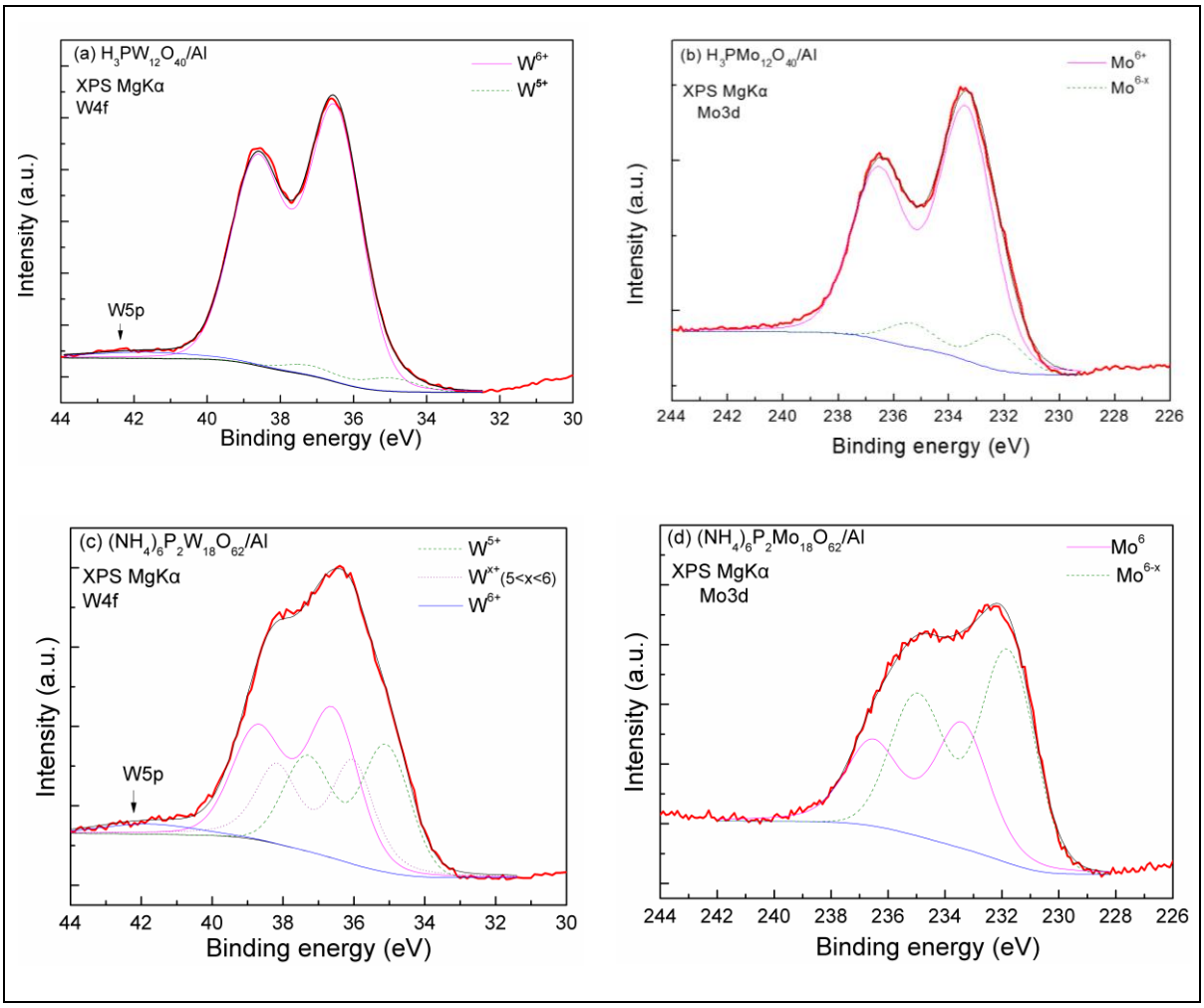

Figure S3. XPS spectra of thick POM films: (a) $H_3PW_{12}O_{40}$, (b) $H_3PMo_{12}O_{40}$, (c) $(NH_4)_6P_2W_{18}O_{62}$, and (d) $(NH_4)_6P_2Mo_{18}O_{62}$, onto Al-coated Si wafers. (POM concentration, 5 mg ml^{-1} in MeOH; drop casting at *RT*; 10-nm-thick Al film; 5-nm-thick SiO_2 film.)

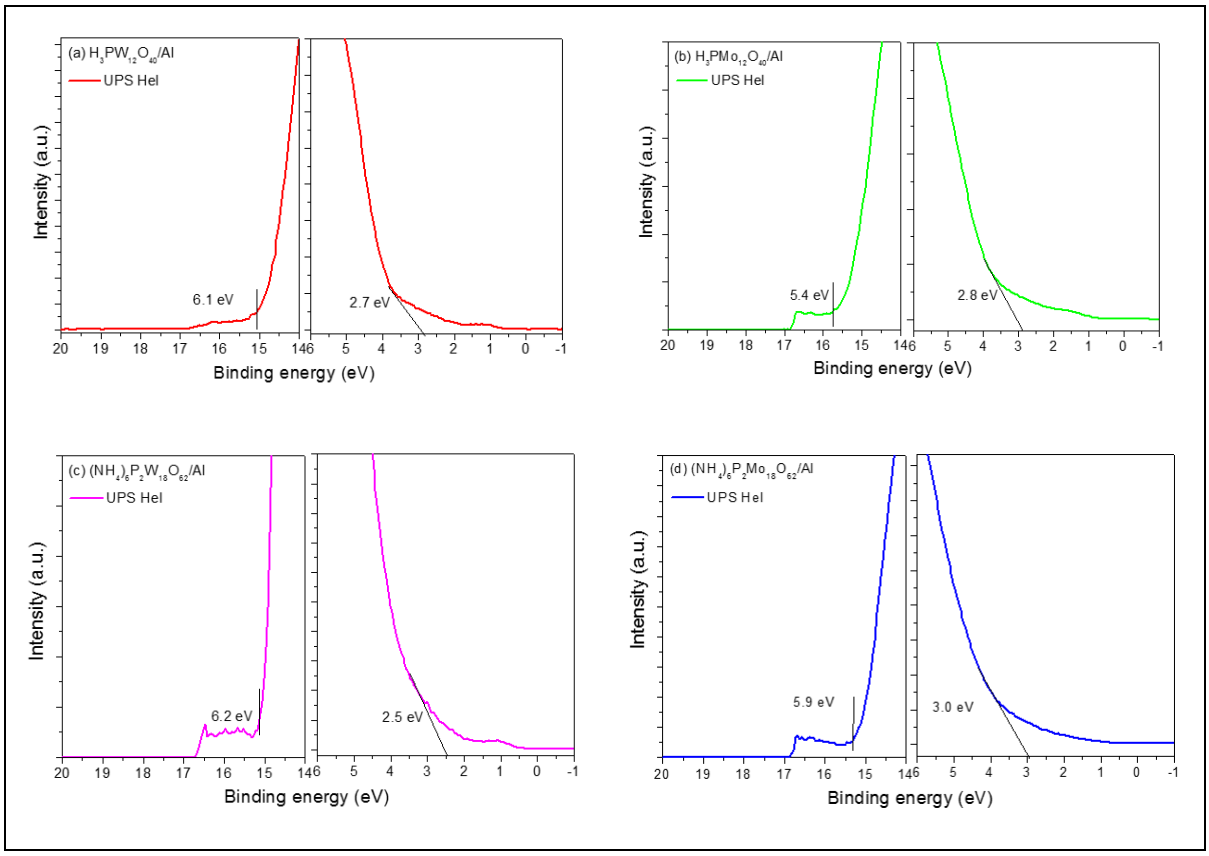

Figure S4. UPS spectra of thick POM films: (a) $H_3PW_{12}O_{40}$, (b) $H_3PMo_{12}O_{40}$, (c) $(NH_4)_6P_2W_{18}O_{62}$, and (d) $(NH_4)_6P_2Mo_{18}O_{62}$, onto Al-coated Si wafers. The work function (W_F) and the HOMO energy level (E_{HOMO}) values of POMs are depicted in the spectra (left and right values respectively). The ionization energy (I_E) value of POMs results from the sum: $W_F + E_{HOMO}$. (POM concentration, 5 mg ml^{-1} in MeOH; drop casting at *RT*; 10-nm-thick Al film; 5-nm-thick SiO_2 film.)

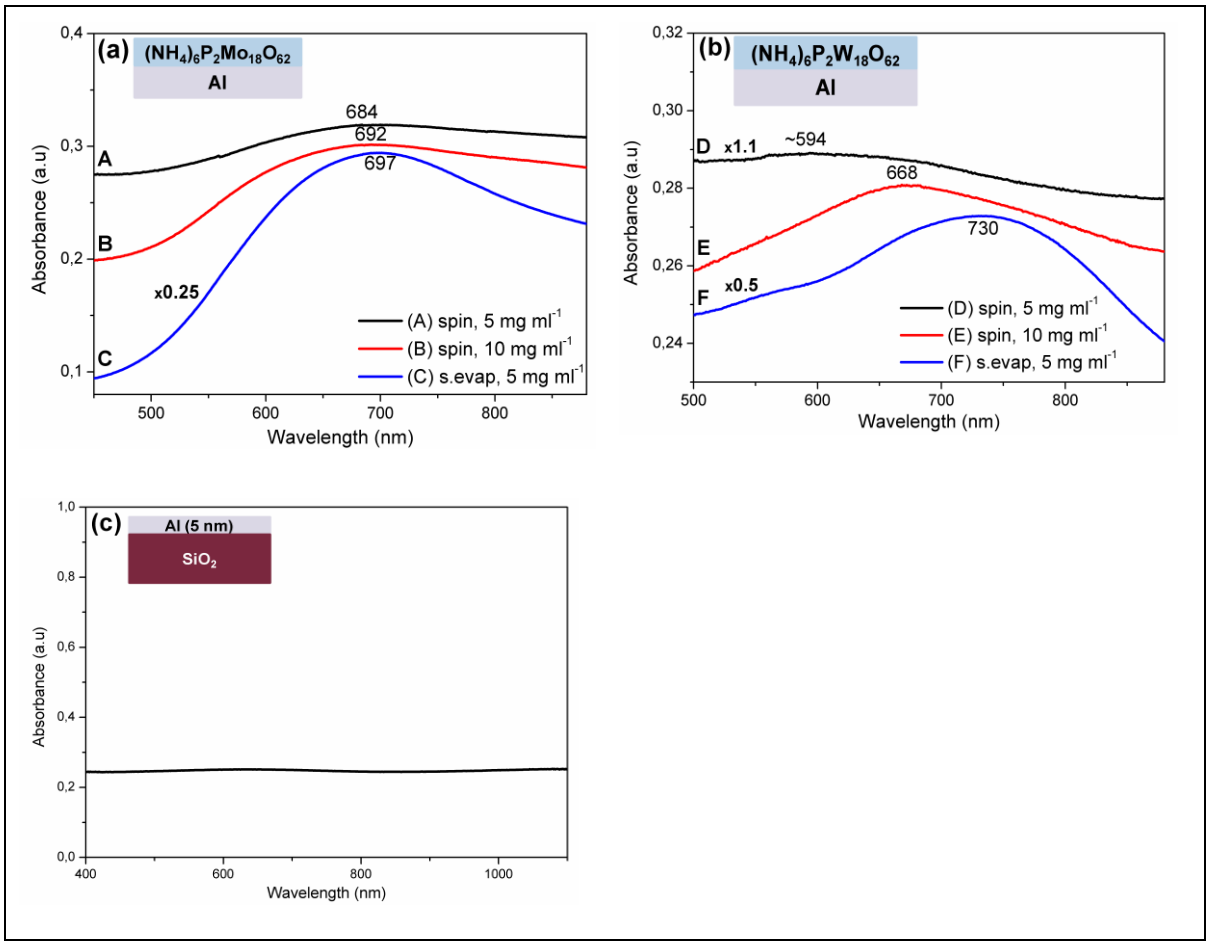

Figure S5. UV-Vis monitoring of POM films: (a) $(NH_4)_6P_2Mo_{18}O_{62}$ and (b) $(NH_4)_6P_2W_{18}O_{62}$, onto Al-coated quartz slides, upon increase of POM film thickness. In all cases the change of IVCT band of POMs is shown. The increase of POM film thickness was realized as follows: (A, D) spin-coating of a 5 mg ml^{-1} POM solution, (B, E) spin-coating of a 10 mg ml^{-1} POM solution, and (C, F) solvent-evaporation of a 5 mg ml^{-1} POM solution. (c) UV-Vis spectrum of an Al–coated quartz slide. (POM concentration, 5–10 mg ml^{-1} in MeOH; spin-coating, 600–700 rpm, 30–40 s; drop casting at *RT*; no thermal treatment applied; 5–10 nm thick Al film.)

The effect of POM film thickness on the reduction degree of $(NH_4)_6P_2Mo_{18}O_{62}$ film onto Al substrate was investigated with UV-Vis spectroscopy (Fig. S5a). As shown in this figure, a ~2nm-thick $(NH_4)_6P_2Mo_{18}O_{62}$ film formed by spin coating of a 5 mg ml^{-1} POM solution, exhibits an IVCT band at 684 nm indicating a reduction degree of ~4e^-. Gradual

increase of film thickness (slightly higher than 2 nm and formed by spin-coating of a 10 mg ml^{-1} POM solution) results in red-shift of IVCT band (684→692 nm) indicating decrease in the reduction degree (2–4e^-).[36,50] A much higher increase of film thickness (e.g. by drop casting of a 5 mg ml^{-1} POM solution) induces further red-shift of IVCT band (692→697 nm) showing additional decrease in reduction degree (2–4e^-). Similar results were also obtained with the increase of $(NH_4)_6P_2W_{18}O_{62}$ film thickness (Fig. S5b), although in that case larger red-shifts of IVCT band and therefore higher decrease in the reduction degree was observed. Thus, it seems that the following general rule is valid: the lower the POM film thickness the higher the reduction degree of Wells-Dawson POMs onto Al substrates.

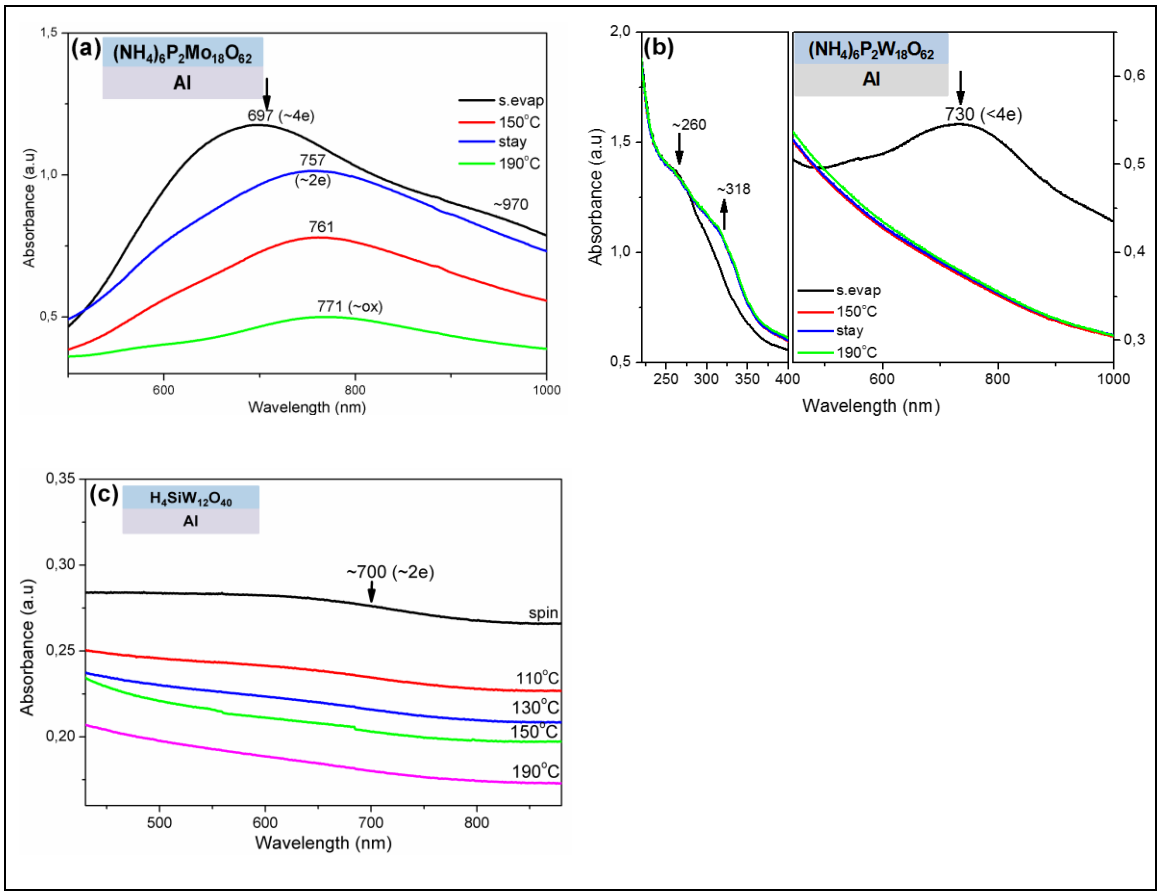

Figure S6. UV-Vis monitoring of POM films: (a) a thick $(NH_4)_6P_2Mo_{18}O_{62}$ film, (b) a thick $(NH_4)_6P_2W_{18}O_{62}$ film, and (c) a thin $H_4SiW_{12}O_{40}$ film, onto Al-coated quartz slides, upon increase of thermal treatment temperature. In (a, c) the change of IVCT band of POMs is shown, whereas in (b) the change of both IVCT and OMCT bands of POM is presented. ((a, b) POM concentration, 5 mg ml^{-1} in MeOH; solvent evaporation at *RT*; thermal treatment in air, at a temperature range of *RT*-190 ^{o}C, for 5 min; stay in air at *RT*, 60 min. (c) POM concentration, 10 mg ml^{-1} in MeOH; spin coating, 700 rpm, 30 s; thermal treatment in air, at a temperature range of *RT*-190 ^{o}C, for 5 min; 10-nm-thick Al film.)

The effect of thermal treatment temperature on the reduction of thick $(NH_4)_6P_2Mo_{18}O_{62}$ film onto Al substrate, was studied with UV-Vis spectroscopy (Fig. S6a). Initially the thick $(NH_4)_6P_2Mo_{18}O_{62}$ film is less reduced (~4e$^-$) than the thin respective film, based on the IVCT band position (697 *vs.* 692 nm respectively; Figs. S6a *vs.* 2a).[7,36,50] Upon increase of thermal treatment temperature, the IVCT band of the thick $(NH_4)_6P_2Mo_{18}O_{62}$ film

decreases in intensity and red-shifts until complete elimination indicating thermal reoxidation of the film (by dioxygen) in a way similar to the thin respective film. Similar IVCT results were also obtained for the thermal reoxidation of a thick $(NH_4)_6P_2W_{18}O_{62}$ film onto Al substrate (Fig. S6b right). Furthermore, upon increase of thermal treatment temperature of a thick $(NH_4)_6P_2W_{18}O_{62}$ film onto Al substrate, a large increase in intensity of the OMCT band at ~318 nm attributed to $O_{b,c}\rightarrow W$ CT is observed (Fig. S6b left) indicating reformation of $W–O_{b,c}–W$ bridges and thermal reoxidation of that film. Similar IVCT band observations were also made for the thermal reoxidation of thin $H_4SiW_{12}O_{40}$ film onto Al substrate (Fig. S6c).[19,45,50]

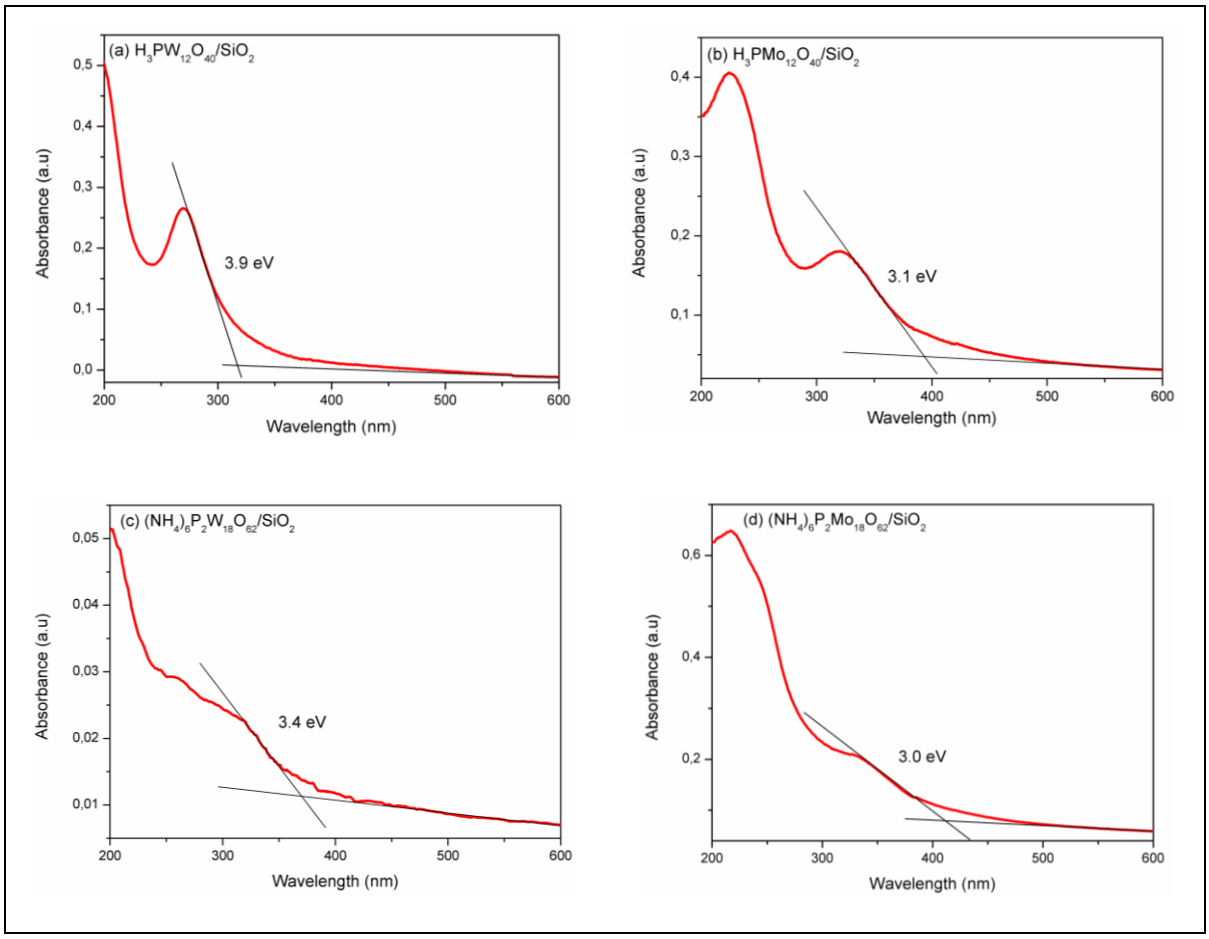

Figure S7. UV-Vis spectra of thin POM films: (a) $H_3PW_{12}O_{40}$, (b) $H_3PMo_{12}O_{40}$, (c) $(NH_4)_6P_2W_{18}O_{62}$, and (d) $(NH_4)_6P_2Mo_{18}O_{62}$, onto bare quartz slides. The energy gap (E_g) value of each POM is calculated from the corresponding spectrum as the ratio of 1240/threshold absorption (nm) of the OMCT band in the near-visible area.[63] POM concentration, 10 mg ml^{-1} in MeOH; spin-coating, 600-700 rpm, 40-120 s; no thermal treatment applied.)

Table S1. Energy levels' values of POMs deduced from the UPS spectra of POM films on Al substrates (Figure S4) and the UV-Vis spectra of POM films on SiO_2 substrates (Figure S7). The LUMO values (E_{LUMO}) of POMs result from the subtraction: I_E - E_g. The energy levels' values in parenthesis are the corresponding values, which were resulted also from experimental measurements (UPS, UV-Vis) and published in a previous publication of our group.[28]

POMs	W_F	E_{HOMO}	I_E	E_g	E_{LUMO}
$H_3PW_{12}O_{40}$	6.1 (5.7)	2.7 (2.3)	8.8 (8.0)	3.9 (3.4)	4.9 (4.6)
$H_3PMo_{12}O_{40}$	5.4 (5.8)	2.8 (2.2)	8.2 (8.0)	3.1 (2.9)	5.1 (5.1)
$(NH_4)_6P_2W_{18}O_{62}$	6.2 (5.8)	2.5 (2.5)	8.7 (8.3)	3.4 (3.1)	5.3 (5.2)
$(NH_4)_6P_2Mo_{18}O_{62}$	5.9 (5.8)	3.0 (2.3)	8.9 (8.1)	3.0 (2.6)	5.9 (5.5)

From the above Table it is observed that almost all the energy levels' values of POMs obtained in the present work are slightly higher than the corresponding values reported in our previous publication.[28] This result was attributed to the higher film thickness and lower homogeneity of POM films in the present case, due to the use of drop casting (instead of spin-coating)[28] as a film coating method of POMs. Anyway, in both cases the trend of the energy levels' values of POMs is the same.

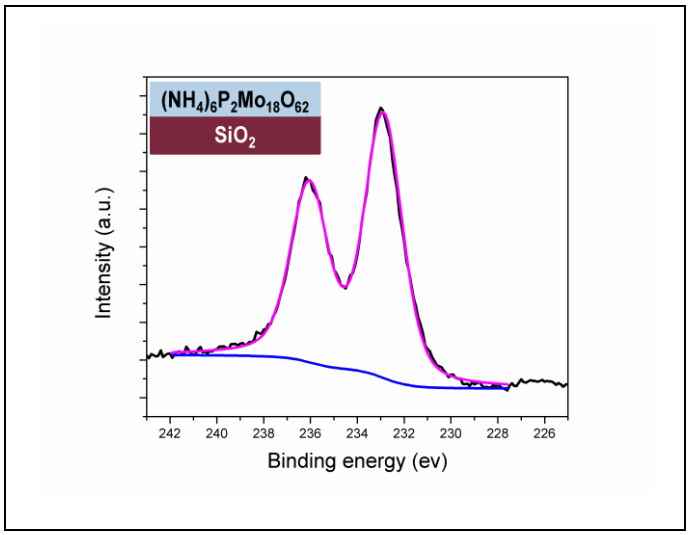

Figure S8. XPS spectrum of a thick $(NH_4)_6P_2Mo_{18}O_{62}$ film onto SiO_2-coated Si wafer. (POM concentration, 5 mg ml^{-1} in MeOH; solvent evaporation at *RT*; no thermal treatment applied; 5-nm-thick SiO_2 film.)

The most reducible Wells-Dawson POM film, $(NH_4)_6P_2Mo_{18}O_{62}$, was found to be in oxidized state onto SiO_2, as shown in its XPS spectrum (Fig. S8).

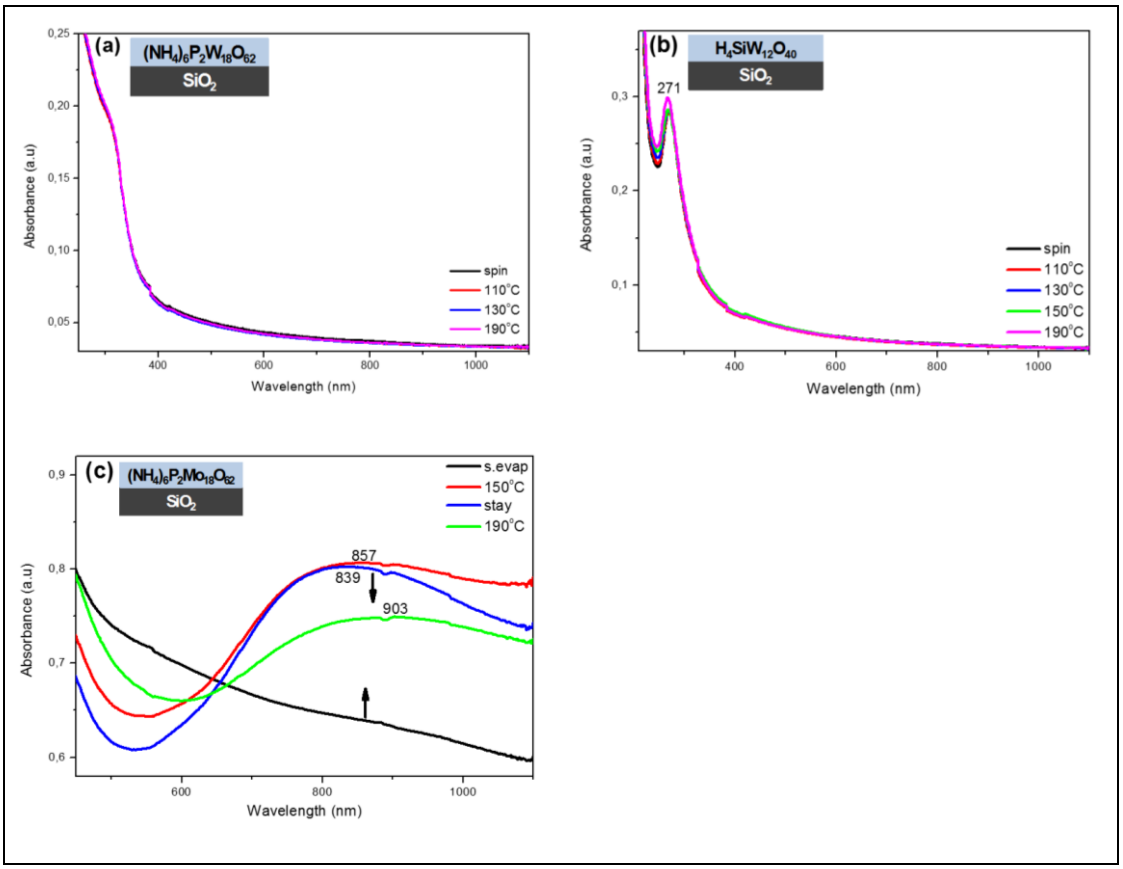

Figure S9. UV-Vis monitoring of POM films: (a) a thin $(NH_4)_6P_2W_{18}O_{62}$ film, (b) a thin $H_4SiW_{12}O_{40}$ film, and (c) a thick $(NH_4)_6P_2Mo_{18}O_{62}$ film, onto bare quartz slides, upon increase of thermal treatment temperature. In (a, b) the whole spectra are presented, whereas in (c) only the IVCT band is shown. ((a, b) POM concentration, 10 mg ml^{-1} in MeOH; spin coating, 700 rpm, 30 s; thermal treatment in air, at a temperature range of *RT*-190 ^oC, for 5 min. (c) POM concentration, 5 mg ml^{-1} in MeOH; solvent evaporation at *RT*; thermal treatment in air, at a temperature range of *RT*-190 ^oC, for 5 min; stay at *RT*, 60 min.)

Upon increase of thermal treatment temperature in thin POM films, $(NH_4)_6P_2W_{18}O_{62}$ and $H_4SiW_{12}O_{40}$, onto SiO_2 substrates, no IVCT band appears indicating that those films are not reduced (Fig. S9a, b). In contrast, the thick $(NH_4)_6P_2Mo_{18}O_{62}$ film is reduced onto SiO_2 substrate upon increase of thermal treatment temperature; though it is reduced to a lower degree (<$2e^-$, based on the IVCT position) than the thin respective film (Figs. S9c *vs.* 6a).